Revista Brasileira de Aplicações de Vácuo, Vol. 11, n. 2, 1992.

PLASMA DEPOSITION OF POLYMER FILMS

R. d'Agostino, P. Favia, F. Fracassi, and R. Lamendola.
Centro di Studio per la Chimica dei Plasmi,
CNR Department of Chemistry, University of Bari 4,
Trav. Re David 200, 70126 Bari, Italy

ABSTRACT:

The basic principles of plasma polymerization processes are examined along with reactor architecture's. Emphasis is given to the chemistry of the discharge and to active species and deposition precursors with the aim of correlating film compositions with discharge internal parameters. The processes for the deposition of films of fluoropolymers, metal containing polymers, SiO_2-likes and silicone-likes, and amorphous carbon are examined as case studies.

1. INTRODUCTION

It has been know for many decades that the introduction of a monomer into a glow discharge, independently of the presence of an inert gas carrier, produces various fragments which rearrange through many gas-phase and surface processes leading to the formation of a variety of addition compounds and of thin films on the inner surfaces of the reactor. For many years plasma thin films were considered an accidental occurrence in hydrocarbon discharges and undesirable by-products to be eliminated. Only after the 60's some researchers showed an interest in their advantageous characteristics [1]. If such films are obtained under controlled conditions, that is, at the desired substrate temperature, gas pressure and electrical discharge parameters, they have unique characteristics allowing their classification as an entirely new class of materials with only small or negligible correlation with their counterparts obtained by conventional techniques.

Good quality plasma thin films have thicknesses ranging from few hundreds Å's to a few μ's, are pinhole free, homogeneous, and show good adhesion to various substrates. The principal structural differences from conventional counterparts are variable stoichiometry (depending on the experimental conditions), higher cross-linking degree and variable chemical-physical properties, such as wettability, chemical inertness, dielectric parameters, barrier properties, hardness, etc.. A typical example is given by Plasma Polymerized Fluorinated Monomers (PPFM) which can be tailored either as Teflon-like with an overall $(CF_{1.9})_n$ stoichiometry (non wettable and inert films), either as partially fluorinated carbon films, *e.g.* $(CF_{0.2})_n$, (high cross-linking and wetable) [1,2], or as a diamond-like film, a-C:H,F [3] (hard, most carbon sp^3 hybridized).

In the remainder of this article characteristics of deposition processes are given (section 2). Reactor geometry will be discussed in section 3. Then, as practical examples, in sections 4 through 7 fluoropolymer, metal-containing, silicon-carbon containing, and amorphous carbon films are examined.

2. GLOW-DISCHARGE POLYMERIZATION PROCESSES

The reaction kinetics involved in glow discharge polymerization are extremely complex and the attempt of abstracting a general picture describing all possible situations would be sterile and misleading. The usual generalization used for conventional polymers can not be used with the same meaning, a particular example being the word "monomer" which indicates the unit molecule repeated in conventional polymeric chains; for instance, polytetrafluoroethylene denotes a polymer in which tetrafluoro-ethylene represents the monomer unit repeated n times in each chain. In glow discharge polymerization, in most cases, the structure of the feed gas is not retained because different radicals, ions, atoms, etc., can be formed in the discharge medium. Nevertheless, the word "monomer" is sometimes utilized in Glow Discharge Polymerization or Deposition simply to denote the feed gas.

Two general considerations on competing processes can, however, be made to describe discharge polymerization, *i.e. etching-deposition competition and gas phase-surface competition.*

2.1. ETCHING-DEPOSITION COMPETITION

It is well known that etching-deposition competition is a rather general phenomenon, some feeds can in fact be utilized in glow discharges both for deposition and etching processes [4]. A well known example is given by SiF_4- and $SiCl_4$-containing feeds, utilized for the deposition of amorphous silicon, a-Si:H, X (X=F or Cl), or for etching of many materials (e.g. Si, SiO_2, Al, GaAs, etc.). Usually atoms, particularly F and O atoms, are regarded as the active species for etching, while radicals are considered "building blocks" for the construction of organic and inorganic films. A glow discharge fed with reactive organic gases produces both types of species. The behavior of freon discharges can fairly well illustrate such competition: the discharge medium contains both classes of active species (F atoms and CF_x radicals), so their concentration ratio $[F]/[CF_x]$ in the plasma phase will characterize their ability as etchant or polymerizing discharges

However, if a gas is added to a freon feed able to reduce [F] in plasma phase, the radical concentration prevails and the plasma is switched into a polymerizing mode. In fact, if hydrogen is added, reacts with F-atoms leading to unreactive HF. Similar conditions can be obtained either by adding to the freon feed an unsaturated, as for instance C_2H_2, C_2H_4, C_3H_6, etc., or by loading the reactor with large silicon surfaces (which react with F, leading to the etch products SiF_2 and SiF_4). On the other hand, if oxygen is now added to freon, it acts both as a polymer etchant and as a polymerization inhibitor: it reacts directly with polymer units leading to volatile compounds or it selectively reacts with CF_x radicals and subtract them from gas phase, inhibiting polymerization process. Figure 1 [4] illustrates the behavior of freon feeds in the presence of different additives.

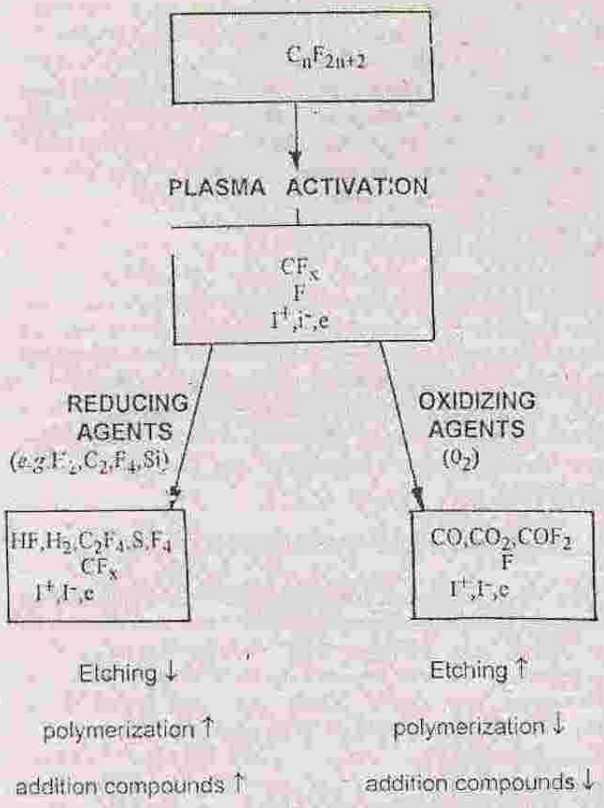

Figure 1. Effect of foreign gas additions to a freon on the etching/polymerizing capability of a glow discharge.

2.2 GAS PHASE-SURFACE COMPETITION

A quite general scheme representing the fate of a "monomer molecule", A, entering a glow discharge is sketched as follows:

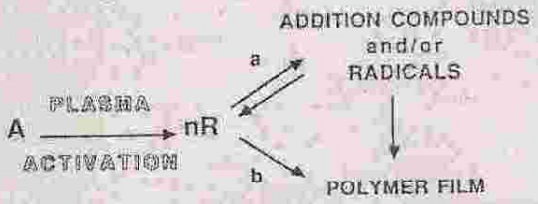

where R represents various radicals. In this scheme A is transformed by plasma activation into various fragments, including atoms, radicals, ions and other molecules.

Radicals (sometimes also atoms) have a two-fold fate: they can, in fact, form addition compounds (branch a) through several reactions paths. These compounds can react in the gas phase with other radicals and unsaturates and form heavier radicals and/or intermediate polymeric chains. Radicals on the other hand, can also contribute to the film growth directly by reacting with "active" surface sites of the film (branch b).

The formation of heavier and heavier addition compounds in reaction I can be enhanced by increasing the production of radicals and decreasing their diffusion to the substrate, in other words, at high powers and/or pressures. In this case, polymer formation can also occur directly in the gas phase through the formation of polymer nuclei. If the radical production is decreased and also their diffusion is increased, route b is triggered and radicals can "stick" on polymer surface directly from gas phase. Generally, the competition between gas-phase formation of intermediate compounds or gas-phase nuclei and surface reaction is frequently met and depends on discharge parameters and feed gases [2, 5-7].

3. REACTORS

The most widely used reactor configurations for Plasma Enhanced Chemical Vapor Deposition (PECVD) can be broadly divided into three classes:

a) electrodeless microwave (MW) or high frequency (HF) reactors,
b) external electrodes "tubular reactors",
c) internal electrodes "parallel plate reactors"

The choice of the experimental arrangement can greatly affect the deposition rate and deposit properties; consequently, it is important to use the experimental system which is appropriate to the specific applications.

3.1 ELECTRODELESS REACTORS

Microwave powered systems are characterized by the use tubular quartz or Pyrex reactors and a resonant cavity coupled with a power supply in the GHz (typically 2.45)

region, as schematized in figure 2. The plasma is generated in the cavity and the deposit is generally collected outside the glow [18-10].

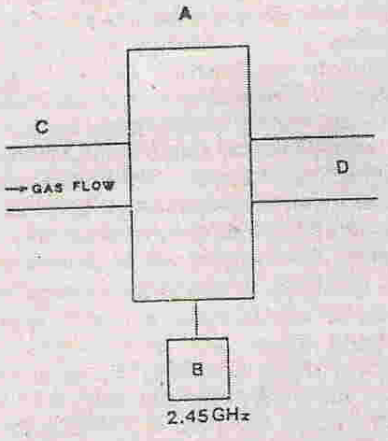

Figure 2. Schematic of a microwave powered tubular discharge: A) resonant cavity; B) generator; C) and D) usual sample position.

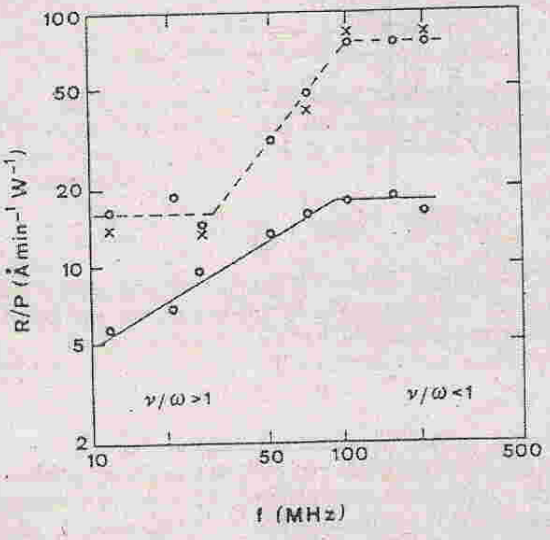

Figure 3. *Log log plot of* (R/P) *vs* excitation frequency. P is the absorbed power and R the deposition rate. The upper curve pertains to PP isobutylene, the lower one PP perfluorocyclobutane.

Claude *et al.*[11-13] and Wertheimer *et al.*[14] have studied the difference between these discharges and RF ones. These authors have used systems connected to an electromagnetic Surface Wave (SW) generator in order to investigate the effect of frequency changes on the deposition processes (e.g. fluorocarbon deposition) keeping constant all other parameters. The ratio of deposition rate R to input power P vs the frequency is shown in Figure 3. It can be seen that R/P increases with frequency, reaching a plateau. The key parameter, however, is the υ/ω ratio, where υ is the effective average electron-neutral collision frequency for momentum transfer, and ω the wave angular frequency (ω = 2pf). These experimental data are in agreement with the theoretical model of Ferreira and Loureiro [15].

The differences between RF and MW discharges can be summarized as follows:

1) the Electron Energy Distribution Function (EEDF) of the glow tends to become increasingly Maxwellian for MW discharges; at the sane time the high-energy tail population increases with decreasing υ/w (MW regime). This leads to a plasma composition with an enrichment of excited species having high excitation threshold energies;

2) the average electron energy slightly decreases with υ/w;

3) MW plasmas are usually characterized by higher density of active species, electrons and ions for the same absorbed power.

Surfaces exposed to MW discharges are subjected to a non intense bombardment of either negative (mainly electrons) and positive (ions) particles, since the sheath potential drop (floating substrate) is quite small and the charged particles can not be accelerated during the applied cycle, which is too short.

Large differences are therefore expected between MW and RF generated thin films due to the different active species production and to the different role played by ions and electrons. Unfortunately, to these authors knowledge, a comprehensive study on this subject has never been performed. An attempt to study these phenomena is reported by Kammermaier *et al.* [8], but the different sample positions with respect to the glow region in MW and RF discharges, makes the comparison of results rather difficult.

3.2.REACTORS WITH EXTERNAL ELECTRODES

External electrode reactors can be either capacitively coupled (Fig.4a); insulating (glass, quartz, or alumina) tubular reactors are usually utilized. The power is transmitted from a power supply to the gas by a capacitor and a coil, respectively. Inductively coupled tubular reactors, when operating at low pressure (p<<1 Torr), are not uniformly coupled to the supply because coupling quality gradually increases with increasing with increasing working pressure [16]. These systems are generally used for experiments in which charged particle bombardment is not one of the major concerns.

When the discharge glows, after a short transient time, the gas reaches an average plasma potential Vp and any insulated surface, in contact with the plasma, reaches a floating potential Vf (always negative compared to Vp). Positive ions are accelerated and again energy, electrons and negative ions are decelerated by (Vp-Vf) when they cross the sheath over a floating surface.

The evaluation of the positive-ions accelerating

potential is not simple, because it depends on the experimental working conditions. However, by keeping constant the other parameters, the accelerating potential can be more easily varied in internal electrode configuration rather than in tubular reactors. As a consequence, charged particle bombardment is less effective in external electrode systems.

Many different experimental arrangements have been reported in the literature, which differ basically in power supplies, reactor geometry, and sample position. The working frequency of the most commonly used power generators ranges from 13.56 to 35 MHz, while tube geometry changes from author to author (see *e.g.* ref. 17-19) and sample position can vary, as it is schematically shown in Figure 4b [17,18], in order to obtain films with different composition and properties.

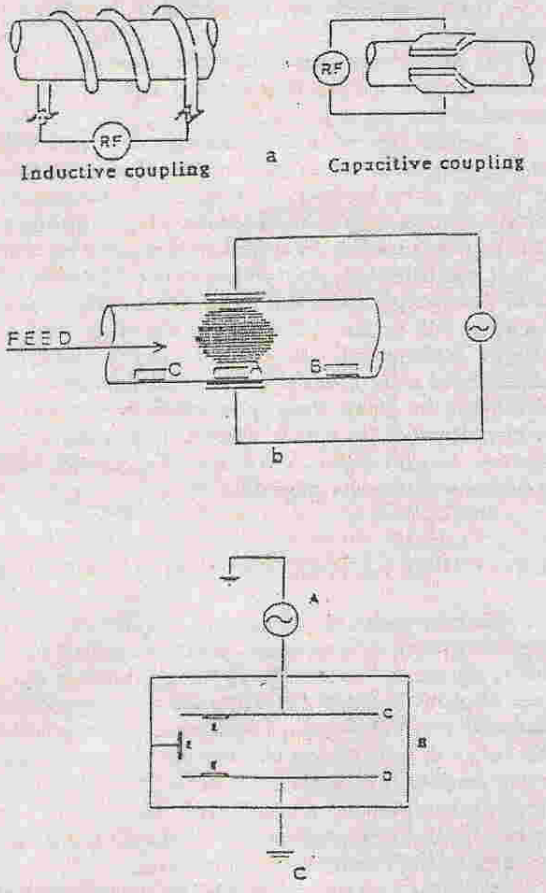

Figure 4. a) Schematics of capacitive or inductive external electrode reactors. b) Usual sample position. c) Internal electrode reactors.

3.3. REACTORS WITH INTERNAL ELECTRODES

Different types of reactors have been developed during the last years, as flat bed, parallel plate, planar, diode, etc. reactors; their main distinctive features are: power supply, coupling system, vacuum chamber, RF driven electrode, grounded electrode and eventually one or more substrate holders (Figure 4c). With these systems, attention must be paid to the appropriate working conditions and geometries, since they can deeply influence the extent of ion bombardment on the substrate (besides, of course, electron energy distribution function and active species production). It is, in fact, reported by several authors [16, 20-22] that the A_t/A_d ratio, where A_d is the area of the driven and A_t that of all other surfaces in contact with the plasma, as well as the coupling system, can affect both V_P-V_F and V_P-V_b, where V_b is the cathode dc self-bias potential (Figure 5A). As a consequence, A_t/A_d affects the energy of ions bombarding floating, grounded, and target surfaces. Increasing A_t/A_d ratio results in increasing the potential drop over the target and in decreasing the potential drop over a floating substrate [22]. An estimation of the average plasma potential V_P can be obtained by $V_P(V_{pp}/2+V_b)/2$ (see Figure 5A), where V_{pp} is the peak-to-peak voltage of the applied RF field [22].

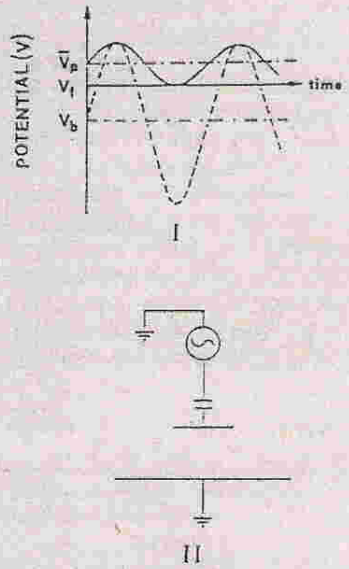

Figure 5A. I) Discharge potentials (p = plasma), f = floating, b = d.c. self bias) evolution. Dashed and continuous curve refer to instantaneous excitation and plasma potential values. II) Schematics of diode configuration maximizing d.c. self bias on target electrode.

Power supplies coupled to reactors with internal electrodes generally work in the KHz or MHz regions. The RF period influences the Ion Transit Frequency (ITF), defined as the frequency above which ions do not cross the sheath in less than half RF cycles. For frequencies below ITF, crossing ions are controlled by the instantaneous plasma potential, while for frequencies above ITF, ions cross the sheath slowly compared

to plasma potential fluctuations, and this leads to an average plasma potential influencing the charged particles arrival to a surface [23]. As a consequence, sharp distributions with a quite low maximum ion energy are expected at excitation frequencies over ITF.

Vacuum chambers can be made either of glass or conductive material, for a better shielding from external sources. In general, there are not particular design problems with the grounded electrode besides its area. On the contrary, the design and arrangement of the cathode require special care; a metallic shield surrounding the electrode highly improves the glow confinement inside the interelectrodic space, and the electrode material and area greatly affect the extent of sputtering on the target.

Asymmetric low-pressure systems ($A_t/A_d>>1$), coupled with high input power, can release large amounts of material by sputtering of the powered electrode. In order to avoid gas-phase and polymer contamination by non volatile material, it could be advisable to work with reactive targets that do not release contaminants. For fluorocarbon deposition, graphite, SiO_2 or teflon targets can be utilized [24, 25]; graphite produces fluorocarbon species and etch products:

$$C + xF \text{ ------> } CF_x \qquad (2)$$

and acts as a fluorine atom scavenger leading to plasma conditions with low F/C ratio [25], a condition which is highly desirable in plasma polymerization. SiO_2 can produce SiF_4 and CO_2 according to:

$$SiO_2 + CF_4 \text{ ----> } CO_2 + SiF_4 \qquad (3)$$

These species, however, do not appreciably change the C/F ratio, but they can change gas phase characteristics and can lead to some film contamination (Si, O). Teflon targets do not affect the C/F ratio, but may require suitable arrangements due to their particular electrical properties.

Substrates are generally positioned on the ground electrode or on a third one (substrate electrode) which can be inserted into the glow. The three electrode arrangement, called 'triode', is very useful for studying the effects of positive ion bombardment on the deposition rate and on film properties. The substrate electrode can be negatively biased with RF voltage by means of a second RF generator [25], or by a capacitive power distribution between the driving and the substrate electrode [26,27], as it is shown in Figure 5B. Since the substrate electrode can be made relatively small in comparison with the main RF electrode, the arrangement allows to change significantly the substrate bias voltage with no appreciable change of total power input in the discharge [28, 29] and, consequently, its chemical composition. In any case a correct approach to the issue of controlling the effect of bias on the deposition is to verify, by means of some diagnostic techniques, the eventual changes induced by bias superposition in the plasma density and potential. Suitable techniques are, for example, Actinometric Optical Emission Spectroscopy (AOES) [30-33] and electrical probe analysis.

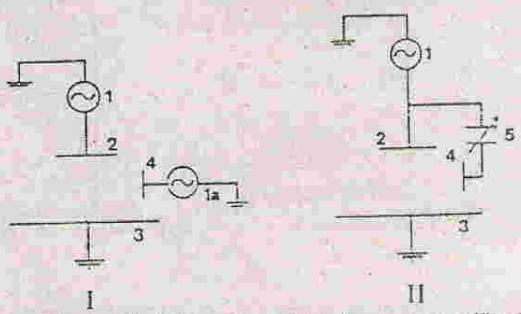

Figure 5B. Schematics of triode reactors utilized for thin film depositions. I) Target (2) and biased deposition electrode (4) are driven by separate RF generators (1,1a), 3 is the grounded surface. II) As for A, but driven by one RF generator with a capacitive power distribution device.

3.4 MAGNETRON REACTORS

Magnetron reactors constitute an important development in devices for plasma-assisted processing of materials. This kind of reactor includes all systems where an additional magnetic field is superimposed to the main electromagnetic field sustaining the discharge. In these systems the electrons under the influence of the magnetic field, follow a spiral path which leads to a decrease of the effective mean free path and to an increase of electron and active species concentration. The scape of the charged particles from the glow region is markedly decreased and a more intense and confined plasma is obtained. Usual problems met with magnetically-aided plasmas (also ECR systems fall in this category) are a higher inhomogeneity of both the growth rate and the chemical composition of the deposited material. The main advantages are a reduced working pressure (about one order of magnitude lower) and a reduced radiation damage of substrates. In fact, there are larger number densities of positive ions hitting the surfaces, but at lower accelerating potentials.

4. FLUOROPOLYMERS

The study of freon-fed discharges has been the object of intensive research in the last decade [4, 6, 7, 34-36], because of their relevance as: a) suitable plasmas to promote etching of a variety of substrates utilized in microelectronic technologies and, b) plasmas allowing the deposition of Plasma Polymerized Fluorinated Monomers (PPFM) films, also said Teflon-like films.

The reasons for the wide utilization of Teflon-like coatings are the good adhesion to many organic and inorganic substrates, the presence of low intermolecular forces, which give rise to relative inert surfaces with extremely low free energy [7], the biocompatibility, the low coefficient [37, 38], and the chemical composition and cross-liking degree, which can be changed in a broad range producing custom-tailored films for protection of a variety of plastics, fibers and metals [1, 2, 7].

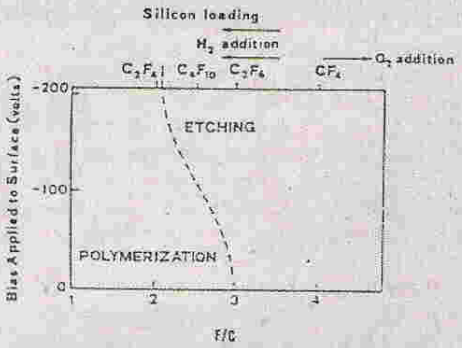

Figure 6. Polymerization and etching regimes as a function of feed F/C and of substrate bias.

The versatility of fluorocarbon plasmas essentially witnesses the ability to produce two kinds of long-lived active species in the discharge, *i.e.* F atoms and CF_x radicals. F atoms trigger the etching of many substrates and allow the fluorination of many organic surfaces, while the radicals form various deposits of Teflon-like films.

Coburn and Winters, and Kay *et al.* [36] have shown that, for discharges fed with fluorine-bearing gases, the fluorine-to-carbon ratio, F/C, of the feed monomer can be used as a simple parameter enabling to keep in perspective the polymerizing and etching nature of the glows. In fact, in Figure 6 it is shown that a discharge can be operated in a polymerizing or etching mode depending on the monomer fluorine-to-carbon ratio, at a fixed bias voltage of the substrate.

The boundary region can be crossed by changing the monomer F/C ratio. This sort of "thumb rule" has been shown to be qualitatively valid because there is a direct quantitative correlation (even though non linear) between the monomer F/C and the plasma-phase concentration ratio $[F]/[CF_x]$, where F atoms and CF_x radicals are the active species for etching and polymerization respectively [4]. The correlation between C/F and $[CF_x]/[F]$ can be appreciated from figure 7 [4], where the relative densities of CF, CF_2, and CF_3 radicals, of F atoms, and of fast electrons (>11 eV) are reported for discharges fed with C_nF_{2n+2} (n = 1-3) and CF_3Cl. Data for the tetrafluoroethylene are also included for comparison.

It can be seen from figure 7 that the density of radicals increases with increasing feed C/F, while the density of atoms decreases. The density of radicals, however, is not linear with C/F. The opposite trends shown by CF_x radicals and F atoms in fluorinated feeds is a direct consequence of the fast recombination process that these species undergo in the plasma, *i. e.* it is impossible to obtain both species in large concentration in the same medium. From the trends of Figure 7, one can classify the various fluorinated feeds on the basics of the expected polymerizing ability with the following order:

$$C_2F_4 > C_3F_8 > C_2F_6 > CF_4$$

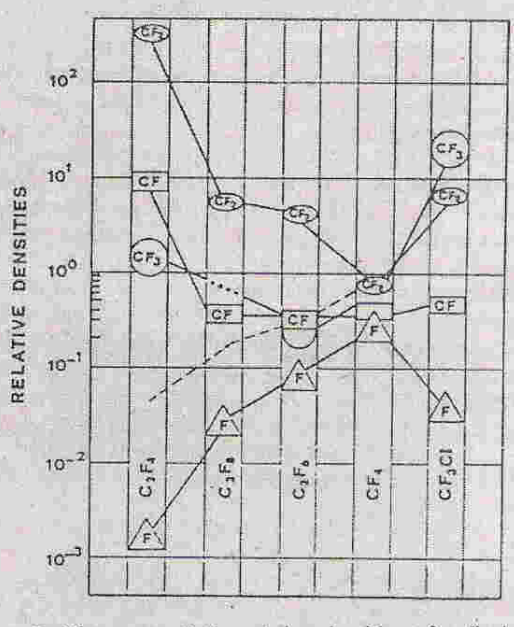

Figure 7. Histogram of the relative densities of radicals, F atoms and electrons (dashed curve), obtained by AOES (see text), for various fluorinated feeds.

Obviously the opposite order has to be expected for the etching ability.

For the aforesaid reasons, the detection and monitoring of active species, as well as the definition of discharge geometries, are important for justifying the deposition of teflon-like films, and allow a non-trivial classification of film properties, as it will be shown later.

Optical Emission Spectroscopy (OES), is generally the most utilized technique for low pressure discharges. In particular, however, Actinometric Optical Emission Spectroscopy (AOES) has been found to be one of the most powerful, non intrusive, diagnostic techniques for monitoring CF_x radicals, F atoms and the trends of electrons at various energies. Since a discussion of AOES is out of the scope of this chapter, readers can make reference to Coburn et al. [39] and d'Agostino et al [32,33,39-43]. Most of data shown in the remainder in this section have been obtained by means of AOES.

4.1.DEPOSITION MECHANISM OF TEFLON-LIKE FILMS

It has been shown [2,4,30-33,44] that a high $[CF_x]/[F]$ ratio in the discharge is not the only sufficient condition to obtain high polymerization rates; two additional conditions are required:

a) plasma media with relatively high density either of fast electrons (> 11 eV) for substrates under floating

conditions, or of positive ions, for biased substrates. This can ensure, due to the bombardment of the surfaces by charged particles, a growth process which occurs through reactions of radicals with activated polymer sites;

b) rather low substrate temperatures. The adsorption-desorption equilibrium of CF_x radicals, which is exothermic, in fact regulates the overall kinetics of polymerization, leading to an *apparent* activation energy which becomes increasingly negative at higher substrate temperatures.

This behavior has been interpreted as a consequence of a film growth mechanism occurring through the reaction of radicals with polymer sites "activated" by charged particle bombardment. A simplified Activated Growth Model (AGM) has been suggested to give account of the experimental results. AGM implies that branch b of reaction (1) in section 2.2 can be represented as:

$$CF_x \xrightarrow{(POL)^*_n} (POL)_{n+1} \qquad (4)$$

where CF_x radicals can stick efficiently *only* on activated polymer surface-sites, $(POL)_n$*, leading to an increase of one unit, $(POL)_{n+1}$. Obviously, activation by fast electrons and positive ions, and termination by neutrals M also occurs:

$$(I^+, e^-) + (POL)_n \text{ ------->} (POL)^*_n \qquad (5)$$

$$(POL)^*_n + M \text{ -------> } (POL)_n \qquad (6)$$

IT an be shown [33], by the use of simple mathematics, that the kinetics equations (4-6) lead to a polymerization rate, R_p, which can be expressed by:

$$R_p = K\,[CF_x]\,f(n_e) \qquad (7)$$

where $f(n_e)$ is a function of charged particles, either electrons or positive ions. Equation (7) has been found to fit experimental data once trends of CF_x radicals and of electrons are obtained by AOES, whatever are feed composition, substrate position and discharge pressure (< 3 torr, otherwise step a of equation (1) in section 2.2 becomes operative), provided substrate bias potential and input power are not so high to trigger the sputter-etching of the film, or the formation of nuclei in the gas phase, respectively.

4.2. FEED COMPOSITION

The effect of feeding the glow with pure freons has been shortly discussed in section 4. It is important to realize, however, that discharge characteristics, particularly $[CF_x]/[F]$ ratio, can markedly be varied by adding to freon feeds variable amounts of different gases, which can act as scavengers of F atoms or of CF_x radicals. Oxygen is a typical CF_x scavenger and its introduction reduces the deposition performances while enhances the etching characteristics. Hydrogen, hydrocarbon and unsaturates, on the other hand, can all produce the opposite effects [30,333,40,45] according to an overall reaction scheme of the type:

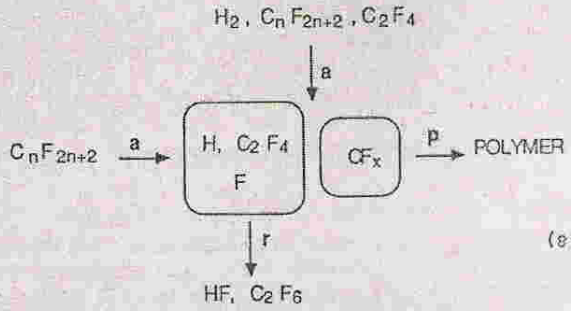

(8)

where step a represent all the plasma activation channels in the presence or absence of plasma additives, step p accounts for polymer formation, and steps r are the recombinative routes, which are particularly important in the presence of additives).

As an example of the good fit to experimental data of AGM, one can examine figures 8 and 9, where trends of plasma active species and polymerization rates, both experimental and calculated according to equation (7), respectively, are plotted as function of percent of hydrogen in a C_2F_6 feed.

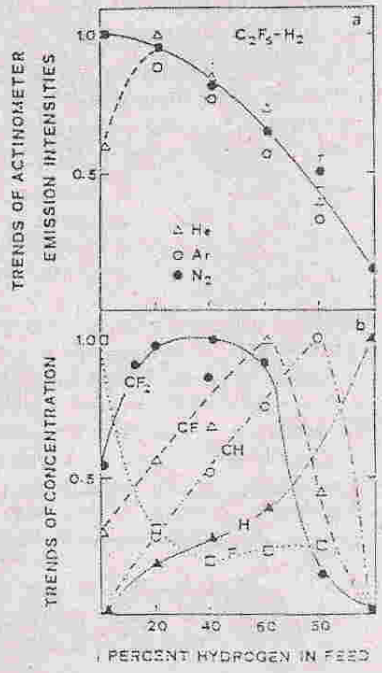

Figure 8. Trends of actinometer (He, Ar, N_2) emissions and of concentrations of radicals ant atoms vs. H_2% in C_2F_6.

When the substrates are placed on a negatively biased electrode [44], the charged particles activating polymer sites are likely positive ions, due to the negative self-bias of target electrodes. Figure 10 [25], obtained in CF_4-C_2F_4 discharges, shows another important effect of positive ions, *i.e.* by increasing the energy of ions impinging on the substrate, a competition of etching and sputtering processes occurs during polymerization. One can conclude that, in the presence of highly energetic ion bombardment, the rate expression for polymerization has to take into account the negative contributions of ion-assisted etching and sputtering:

$$R_p=K_p\,[CF_x]f[I^+]-K_e[F]g(I^+)-K_{sp}\,h(I^+) \qquad (9)$$

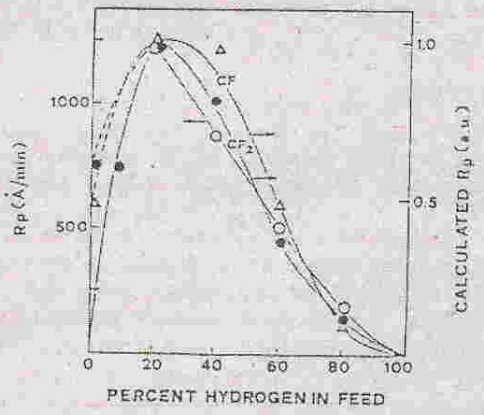

Figure 9. Comparison of experimental (open circles) and calculated (by means of AGM; black circles - curve obtained by using the experimental CF_2 trend; triangles- curve obtained by using CF trend) polymerization rates *vs.* H_2 % in C_2F_6.

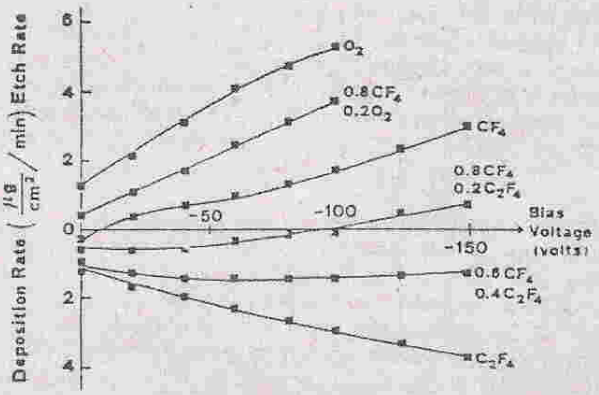

Figure 10. Deposition and etching rates *vs* bias voltage for different CF_4-C_2F_4 mixtures.

4.3. THE EFFECT OF SUBSTRATE TEMPERATURE

It has been shown [2] that, when polymerization occurs on a floating substrate immersed in the glow, the substrate temperature increases from room temperature up to 150°C, for discharges fed with C_2F_6-H_2 mixtures at 300 mtorr, 25 sccm total flow, and 45W. Under these conditions, it has been reported that instantaneous polymerization rates continuously decrease and are characterized by two main features:

1) Rp's do not show an Arrhenius type behaviour because of the apparent negative activation energy;

2) at lower temperatures the apparent activation energy is close to zero.

A competition between two regimes, an adsorption-desorption equilibrium and a chemical surface reaction, can account for this behaviour:

$$CF_x\,(g) \rightarrow \quad CF_x\,(surf) \qquad (100$$

$$CF_{x\,(surf)} + SS \rightarrow POLYMER \qquad (11)$$

in which SS of equation (11) are surface sites which can generate a polymer unit.

This formulation is not in contrast whit AGM; it is, in fact, sufficient to consider physical, (10), and chemical, (11), contributions.

4.4. THE CHEMICAL STRUCTURE OF TEFLON-LIKES

The most attractive feature of plasma polymerized films and, in particular, of PPFM, or Teflon Like, coatings is the large range of compositions and structures and the possibility of controlling its variation by means of external plasma parameter, *e.g.* feed composition, bias superposition and power density, which affect CF_x radical distribution and charged particle bombardment. X-ray Photoelectron Spectroscopy (XPS or ESCA) is the most utilized technique to investigate the PPFM film chemical structure, because of the large differences in electronegativity between F and C. As a consequence, photoelectrons emitted by C1s display a broad overall spectrum which is the result of the superposition of several components with different binding energies (BE). Usually, decomposition procedures are available which allow an unambiguous deconvolution of the overall spectrum.

The peak centered at 285.0 eV can be due either to carbon not directly attached to fluorine, having no β fluorine substituents, or to -CH groups. In some cases, the contribution of quaternary carbon is predominant. PPFM stoichiometry can be easily calculated either by the total integrated intensity of F F1s and C1s or by the distribution of the integrated intensities of the various components of C1s spectrum. It is also important to notice that the integrated intensity of -C-CF and -C- components, with respect to the overall C1s, is a direct measurement of the degree of branching and cross-linking of the polymer films.

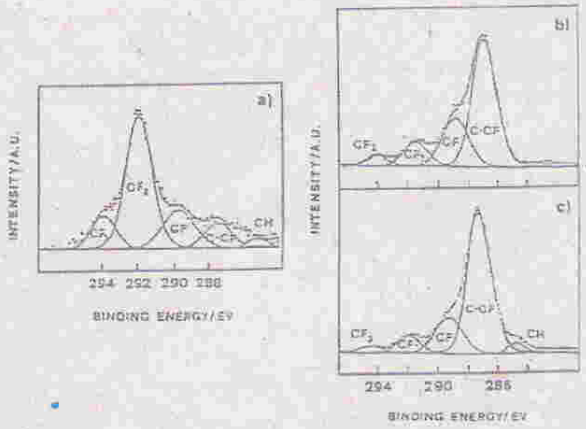

Figure 11. XPS C1s spectra of films deposited at various H_2% in C_2F_6: a) 20%, b) 50%, c) 70%

Main features of these spectra are [2,46-48]:-CF_3 (BE=294.0 eV),-CF_2 (BE=292.1 eV),-CF (BE=294.0 eV),-C-CF (BE=287.3 eV), and -C- (BE=285.0 eV)as shown in figure 11.

The continuous addition of hydrogen to a discharge fed by a perfluorinated freon, by keeping constant both pressure and total gas flow rate, causes a variation of film structure as it can be seen from figures 11 and 12.

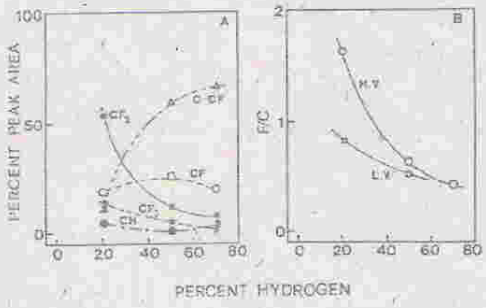

Figure 12. Relative abundance of carbon groups and overall F/C ratio of the films *vs.* H_2% in C_2F_6.

Figure 12 shows that the hydrogen addition to inlet C_2F_6 changes the overall film stoichiometry and the component distribution by progressively favouring less fluorinated film compositions, film branching and cross-linking. These results should be compared with those of Figure 8 where the hydrogen effect on gas phase radical distribution mirrors the effect on film components. In fact, also in the gas phase less fluorinated radicals are favoured. Obviously, the relative abundance of film components can not be a simple "photography" of the gas-phase radical distribution because of ion and/or electron bombardment on the film. Such an effect is shown in Figure 12B where H.V. and L.V. traces refer to film obtained at high and low voltages, respectively, under the same power input. This means that the trace marked with L.V. is obtained at higher current density, *i.e.* higher charged particle bombardment. It is evident that charged particle bombardment favours a reduction of F/C ratio and an increase of cross-linking in PPFM films. It can be shown that power input has a similar effect on PPFM chemical structure [6].

5. METAL CONTAINING POLYMER FILMS

Some of the unique characteristics of plasma deposited organic films, as for instance chemical inertness, hardness, and low friction, can be combined with the characteristics of metal deposited films, as electrical conductivity, by generating an entirely new class of materials: the plasma deposited metal-polymer composites. Recently some reviews appeared on this topic [49-52]. From the structural point of view, the principal difference of these composite films with plasma polymerized organometallics is that in metal-polymer composites one deals with a metallic dispersion in an organic matrix, while in organometallics metals are chemically bonded with carbon and/or other species (see § 6).

An interesting feature of plasma metal-polymer composites, from the point of view of the properties, is that, depending on the concentration of metal clusters, one has a dielectric behavior of the films when metal particles are well separated each other, a metallic behavior when these are interconnected, and an intermediate behavior in the percolation region.

Both hydrocarbon and fluorocarbon originated polymer films are widely utilized for metal-polymer composites, and there are also interesting cases of amorphous carbon-metal composite films [51]; usual metals are Au, Al, Co, Pt. Our attention, however, will be here devoted mainly to Au-fluoropolymer films.

Two major systems have been mostly utilized for Au-PPFM films, *namely*, systems with simultaneous plasma polymerization and metal evaporation. In both cases, the most utilized configurations are diode reactors with substrates on grounded electrode. Usually for amorphous carbon films the substrates are placed over the cathode to enhance self-bias conditions. Recently, a triode configuration has also been utilized in order to allow sputtering of the metal target and to observe the effect of substrate bias [53].

The relative Au/C ratio for a fluoropolymer film obtained in a diode reactor with target sputtering depends on the relative gas-phase abundance of the active species for deposition, *i.e.* Au atoms and CF_x radicals. The gas-phase [Au]/[CF_x] ratio is, in turn, affected by Au-sputtering, when the other parameters are kept constant. This can be accomplished either by increasing the self bias potential of the target or by feeding the discharge with Ar, besides fluorocarbons, in order to increase the sputter yield of targed metal.

Monitoring of the ratio of the emission intensities of gold line (267.6 nm) and CF_2 band (265.0 nm) revealed to be an useful *in situ* measurement of the gas-phase $[Au]/[CF_2]$ ratio, linearly related to the actual Au/C film composition [54], as it can be seen in Figure 13.

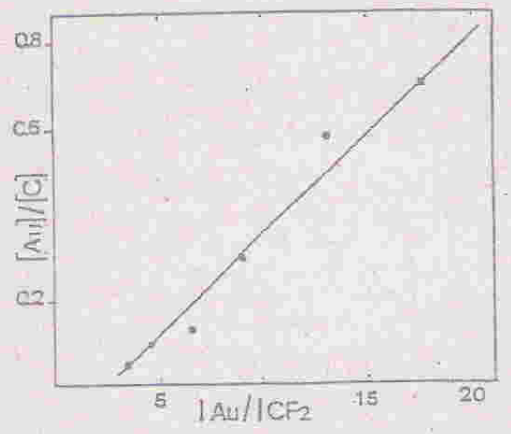

Figure 13. Atomic film composition *vs.* the ratio of Au and CF_2 emission from discharge.

5.1. MECHANISM OF DEPOSITION

The microscopic mechanism of deposition is rather complex and involves several possible steps in the reaction route from the gaseous monomer unit and the metal to the formation of the metal-polymer composite. Both metal atoms and polymer building blocks are to be formed (independently) in the gas phase; they have then to diffuse to the deposition substrate, where the deposition can be differently affected by the bombardment with positive ion of different energies. A possible simplified reaction scheme is the following:

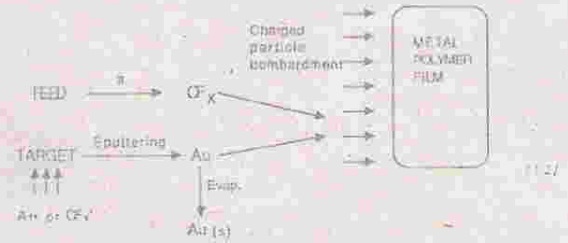

where step a is the plasma activation. Martinu *et al.* [55] have shown, by utilizing probe measurements, that there is a considerable density of negative ions with Au target (with respect to Al target) which "could affect" the deposition occurring on the ground electrode, since they claim that negative ions can be accelerated by a negative potential drop at the target when the electrodes face each other. On our opinion, however, such a chance seems remote in that both electrodes are *always negative with respect to the glow potential*, whatever is the discharge architecture.

On the order hand, in ref. [53], where it was possible to bias the deposition electrode, it has been shown that positive ions do certainly effect the deposition process. In particular, when highly energetic ions are utilized, the Au/C, Au/F and C/F ratios of the film increase and also the chemical structure of the polymer matrix becomes more and more cross-linked.

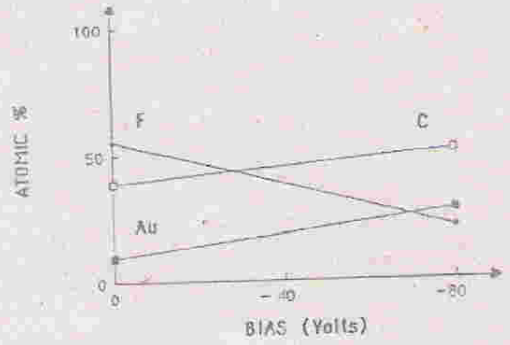

Figure 14. Atomic film composition *vs.* substrate bias (Ts = -13°C).

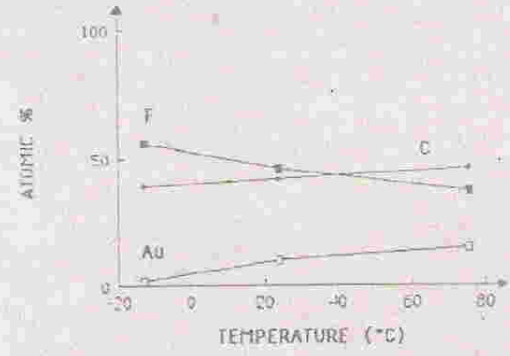

Figure 15. Atomic film composition *vs.* substrate temperature.

This bias effect on the polymer composition can be seen in Figure 14 [53], where the growing film was kept at a constant nominal temperature of -13°C. It is interesting to notice that also the temperature of the substrate affects the chemical composition of the growing film in a similar way. In Figure 15 [53], it is shown that by increasing the nominal substrate temperature from -13°C to + 75°C, Au/F and C/F ratios of the film increase, too. This effect can be due to the longer exposition of the film surface to the ion bombardment at the higher temperatures since the film growth is decelerated (see § 4.3) because of the exothermic adsorption-desorption equilibrium of CF_x radicals.

Finally, it should be mentioned that Kay *et al* [56] have proposed that an polimerization may occur by addition of CF_2 radicals. In this case, the route to polymerization in equation 12 should include $(CF_2)_n$ as intermediate to the polymerization, even though this route should be operative only at the higher pressures, as discussed in section 2.2.

5.2. STRUCTURE AND COMPOSITION OF Au-CONTAINING FILMS

Electron microscopy, ESCA and IR spectroscopy are the principal diagnostic tools which give an insight on film microstructure and composition.

The principal parameters which characterize metal-polymer composites are: the filling factor f, which is defined as the volume fraction of the metal contained in the unit volume of the film, the atomic composition (see figure 14 and 15), and the relative abundance of the various chemical components of the film.

Structural studies have shown that gold grains are randomly distributed in the polymer and their average diameters are in the range of 5-50 nm in the dielectric region (f < 0.4). At larger filing factors there is a dispersion of smaller grains among larger irregular particles. At still larger f (metallic region) there is a complex morphology of grainforms, which start to become more *wormlike* and interconnected.

Annealing seriously effects grain morphology because it increases the motion of gold particles in the relatively soft polymer matrix (particularly at temperature higher than the glass transition of PPFM, around 160°C); then one has a coalescence of particles coming into contact. This characteristic of Au containing PPFM films could seriously affect the utilization of this material due to aging effect. However, in ref. 53 it has been shown that crosslinking the polymer largely reduces this effect. This can be done by increasing the substrate bias and/or temperature during deposition. Going further in this direction, one can reach the conditions for amorphous carbon including metal particles, provide F abstraction is also ensured in the gas phase, either by using monomers with low F content or by adding hydrogen to the monomer feed [53].

5.3. FILM PROPERTIES AND APPLICATIONS

Plasma deposited metal-polymer films feature two important properties: an anomalous optical absorption in the visible and a conductivity response, both being a function of the filling factor.

The optical transmission of films obtained by Au and chlorotrifluoroethylene (CTFE) co-deposition, shown in Figure 16 [57], exhibits a typical minimum, due to optical resonance, the intensity and width of which are a function of the gold volume fraction and grain distribution and morphology. It can be seen that the minimum at 0.55 μm

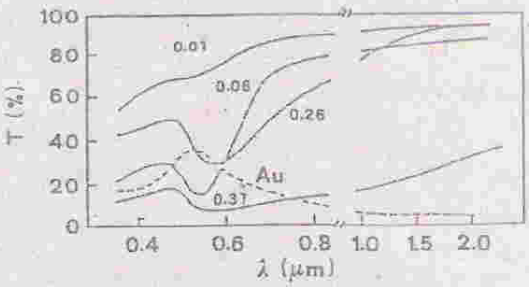

Figure 16. Optical transmission in the visible and near IR regions for gold-doped plasma deposited CTFE films with different metal volume fractions.

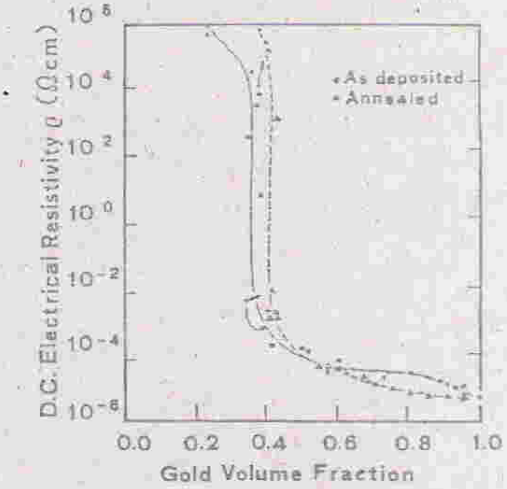

Figure 17. Resistivity variations (four point probe) *vs* gold volume fraction for as-deposited and annealed plasma polymerized C_3F_8 films. Arrows indicate resistivities of films close to the percolation threshold upon annealing to 200°C.

intensifies and shifts with f. Therefore typical film color of gold-halocarbon films are pink (f = 0.02), red (f = 0.1), violet (f = 0.25), and blue (f = 0.4). Green is typical of sputtered gold films.

The electrical conductivity of Au-PPFM films is determined also by f and by metal grain distribution and shape. It can be seen from figure 17 [58] that the resistivity decreases with f, and shows a dramatic drop of about 8 orders of magnitude when f reaches 0.37 (which corresponds approximately to the percolation threshold [58, 59]. It is also interesting to see that, after annealing at 200°C, the resistivity curve shifts toward higher f (the percolation threshold increases from about 0.40 to 0.42), as it should be expected on the basis of the discussed aging of metal composites due to mobility and coalescence of metal grains. On the other hand, if the deposited organic matrix is amorphous carbon, one expects a more rigid behavior and less pronounced optical and electrical variations with both time ad temperature. Such

results can be obtained with gold-PPFM films deposited at higher substrate temperatures and/or bias voltages. A reduction of the aging effect is also observed if the film is post-annealed at T > 200ºC.

For such films interesting applications have been suggested as decorative coatings [60], optical filters [61] and humidity sensors [62]. Morita and Hattori [63] and Hori et al. [64] suggested the utilization of Au-plasma polymerized Styrene composites for a completely dry lithographic process. Kay suggested their utilization for optical recording [65].

6 FILMS FROM SILICON-CONTAINING ORGANIC MONOMERS

Silicon-containing organic compounds, called 'silorganic' monomers, are utilized in PE-CVD of Si-C alloys, silicone-like polymers, silicon oxide and nitride coatings. The composition of the coatings (*i.e.* O/Si ratio, nitrogen and/or carbon content), as well as their properties, depend on the choice of the monomer and on the deposition parameters [66-71]. In order to deposit silicone- and silicon oxide-like films, widely used in optics, bio-medical applications, microelectronics and so on [66], the monomers are usually fed in variable percentages with oxygen or other oxidant gases (CO, N_2O, etc.), whose abundance turns out to affect films deposition rate and chemical composition. In the remainder of this work Tetramethylsilane (TMS), Hesamethyldisilazane (HMDSN), and Tetraethoxysilane (TEOS) monomers will be compared, and it will be shown how the nature of the obtained films can be shifted from an "organic" character (silicone-like structure) into a more "inorganic" one (*i.e.* SiO_2) by increasing one or more of the following process parameters: oxygen per cent in the feed, substrate temperature, and substrate bias. Results regarding a fluorinated silorganic are also included.

6.1. THE EFFECT OF OXYGEN ADDITION TO THE FEED

When oxygen is added to the feed, the deposition rate and the composition of the coatings are influenced (figure 18), due to the reactivity of oxygen molecules and atoms in homogeneous and heterogeneous reactions [67,72]. Film chemical nature, as well as its growth rate, mirrors the precursor distribution in the plasma, which is affected by the oxygen content in the feed.

The overall deposition process can be schematized by assuming that two 'classes' of film precursors can be formed by plasma activation: the "inorganic" precursors, which *contain silicon* along with other elements (e.g. SiC_xH_y, $SiC_xH_yO_z$, etc.), and the "organic" precursors, which do not contain silicon. Even though this distinction can be only a matter of jargon, it can be useful in order to rationalize the deposition mechanism as follows:

Step a - Monomer and oxygen fragmentation (electron impact), *i.e.* formation of organic and inorganic precursors, and of oxygen atoms and excited molecules.

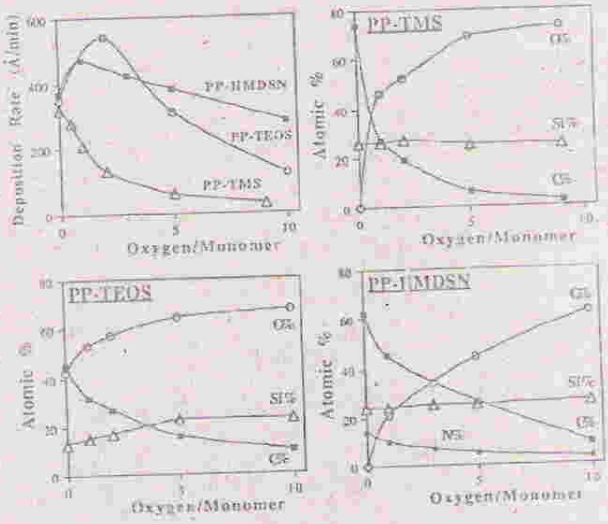

Figure 18. Deposition rates and XPS-measured compositions of coatings obtained by various monomers in mixture with oxygen. PP-TEOS films were analyzed after exposition to the atmosphere, and show an overestimated carbon content.

Step b - Homogeneous reactions between oxygen species and precursors, which modify their distribution depending on the feed oxygen content. These reactions result in scavenging organic precursors, and in decreasing the organic character of the inorganic ones. Byproducts are non polymerizable species, such as CO, CO_2, H_2O. It is important to notice here that the increased feed oxygen-to-monomer ratio usually results in an increased electron density, as it can be revealed by means of AOES [6], which also could be responsible for modifications of the monomer fragmentation paths.

Step c - Polymerization of the adsorbed precursors on the substrate surface.

Step d - Heterogeneous surface oxidation of the growing film by oxygen atoms, and formation of $-SiO_x$ and $-CO_x$ functionalities [67-69,71].

The deposition rate of PP-TMS decreases by increasing the feed oxygen content, while those of PP-HMDSN and PP-TEOS are characterized by a trend with a maximum. These differences can be ascribed to the different importance of process of steps a, b, and c, depending on the type and density of precursors, and/or on the structure and composition of monomer (*i.e.* presence or absence of oxygen and nitrogen). On the other hand, the composition trends of PP-films as a function of the oxygen-to-monomer ratio are similar for the three monomers, and agree with reactions a-d.

XPS and FT-IR analyses have shown [67,69] that, when no oxygen is added to the feed, PP-films are characterized by stoichiometries close to those of monomers, but with different distribution of functional groups, and a lower carbon and hydrogen content. By increasing the oxygen per cent, the following modifications occur which, in effect, can be considered as general:

Carbon - Its abundancy decreases on the basis of reactions b, the decrease is steeper in PP-TMS. The detailed C1s XPS spectra show that the concentration of oxygenated functionalities increases.

Oxygen - Its concentration increases, the shape and position of XPS peak remains almost unchanged.

Silicon - Its content in the film is practically unchanged, however, Si2p peak shifts to higher binding energies for the formation of silicone-like $(C_x\text{-}Si\text{-}O_y)_n$ structures. When a high O/Si ratio is obtained (ratios higher than 2 are due to Si-OH groups), the binding energy reaches its maximum (103.5 eV). It is interesting to notice that Si2p FWHM (mainly in PP-TMS, but also in PP-HMDSN) has a trend with a maximum, which mirrors a continuous composition change in the material with the increase of the feed oxygen content. Films with a "monomer-like" stoichiometry are deposited when no O_2 is added (Si-H, Si-C, eventually Si-N bonds in the film), while "silicone-like" (Si-O plus the aforesaid bonds), and "oxide-like" films (practically only Si-O bonds) are deposited at low and medium-high oxygen-to-monomer ratio, respectively.

Nitrogen - It is always present in PP-HMDSN films and the binding energy of N1s slightly increases with oxygen addition to the feed.

6.2. THE EFFECT OF SUBSTRATE TEMPERATURE AND BIAS

As for fluoropolymers, substrate temperature and bias influences plasma-surface interactions in PECVD from silorganics, by affecting the adsorption-desorption equilibrium of precursors and etchants (whatever they are) heterogeneous reactions, film pyrolysis, and by triggered ion-assisted etching or sputtering processes, depending on ion energy (see section 4 and ref. 66).

Figure 19 shows the effects of substrate temperature on the growth rate of PP-TMS and PP-TFC films, where TFC is a fluorinated silorganic, namely the trimethyil tri(trifluoro n-propyl) cyclo tri-siloxane [71]. The temperature enhancement decreases deposition rate also due to film pyrolysis, which plays a fundamental role in PECVD of organosilicons, as evidence by Wrobel et al. [66]; the pyrolysis breaks Si-H, Si-CH_3 and C-H bonds, leading to crosslinked films. The overall effect on film composition, witnessed by ESCA and FT-IR analysis, are the increase of the Si per cent, and a dramatic decrease of C and H content, whatever is the monomer. In PP-TMS, film density increases from about 1.1 to about 2.0 g/cm^3 for a temperature increase from 60 to 320°C [70].

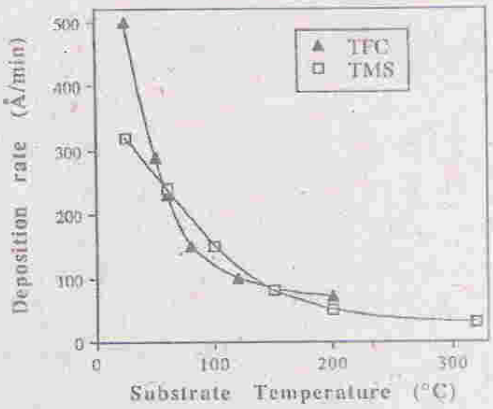

Figure 19. Deposition rate of PP-TMS and PP-TFC *vs* substrate temperature.

In figure 20 the deposition rate of PP-TFC and PP-TMS films (at 200°C) are plotted as function of the substrate bias. Here both the activating and the disactivating effects of ion bombardment, discussed in the previous sections, are shown. Depending on film structure and ion energy, the ion-bombardment can enhance or depress the growth rate; this behavior can be attributed to the competition of two processes triggered at different energies:

a - Low-energy ions enhance film growth rate by creating surface "active sites"(dangling bonds, distortions), more reactive towards precursor radicals. This mechanism is described by the Activated Growth Model (see section 4).

b - High-energy ions assist film sputter-etching (at about -30 V the effect becomes evident for PP-TMS) with etchants, e.g. hydrogen or fluorine.

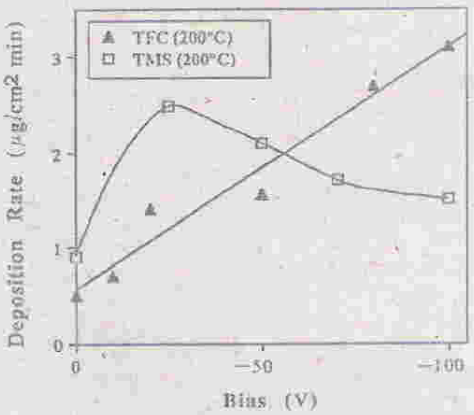

Figure 20. Deposition rate of PP-TMS and PP-TFC *vs* substrate bias (at 200°C).

The bias effects, generally close to those of the temperature (more inorganic, cross-linked, hard, and dense coatings) can be exploited to design films with different structures. Low substrate temperature and bias lead to films whit high monomer-structure retention, while the increase of ion bombardment and/or temperature drives the deposition toward "more inorganic" materials.

7. AMORPHOUS HYDROGENATED- AND FLUORINATED-CARBON FILMS, a-C:H,F

A great deal of work has been produced in the last few years in the field of hard amorphous carbon and diamond films [73-75] because these materials are considered of strategical importance for different applications. The main properties which charm solid state chemists, physicists and engineers can be resumed in hardness, density, chemical inertness, optical transparency, thermal conductivity, dielectricity, semiconductivity [76-79]. Obviously, many investigators have utilized Plasma Enhanced Chemical Vapor Deposition as a tool for obtaining both diamond and diamond-like films, mostly with hydrocarbon-hydrogen mixtures as feeds [76]. On the other hand, some efforts have also been made with hydrocarbon-fluorocarbon mixtures for obtaining amorphous hydrogenated and fluorinated carbon films, a-C:H,F [78-80]. We have utilized C_2F_6-H_2 mixtures [3], as for Teflon-like films, because the highly crosslinked nature of the obtained films (see § 4.4) was encouraging. Our experiments, however, have been performed with a higher dilution level than in mixtures for Teflon-likes: namely, 0-20% C_2F_6-H_2 mixtures fed a triode reactor (in order to analyze the effects of bias and substrate temperature). It is interesting to notice that, under these new conditions, a novel deposition chemistry takes place in the discharge. In fact, while the precursors for Teflon-likes are CF_x-radicals and the film fluorination level depends on the extent of fluorination of the active radicals (i.e. x in CF_x), the conditions used for obtaining a-C:H,F trigger C-atoms and CH-radicals as active species for the deposition and the fluorination level turns out to depend fairly well only on the gas phase concentration of F-atoms.

7.1. FROM TEFLON-LIKES TO a-C:H,F: SWITCHING FROM A CF_x CHEMISTRY INTO ONE BASED ON C- AND F-ATOMS AND CH-RADICALS

In order to investigate the effects caused by the contaminations due to cathode sputtering in discharges for amorphous carbon, the experiments have been run both with graphite and steel cathodes. In figure 21 A the relative actinometric trends of H- and F-atoms, as well as of CF_2-radicals, are plotted as a function of C_2F_6 percentage in the feed. The trend for these species is unaffected by the cathode material. It can be seen that the F-atom density linearly increases with C_2F_6 addition, as it can be expected. However also H-atoms increase, probably because of some reactions involving vibrationally excited species. In figures 21 B and C the profiles of CH-radicals and C-atoms, respectively, are compared in the presence of the graphite and steel cathodes. It can be seen that with the graphite cathode the density of CH-radicals is unaffected by C_2F_6 addition, probably because this species can be produced also by graphite etching induced by H atoms and by sputtering and successive reaction of C with H in the gas phase. On the other hand, C-atom trends do not significantly differ changing the cathodic material, but for the intercept value obtained with graphite (which, again, points out to graphite sputtering as an additional source of carbonaceous species in the gas phase).

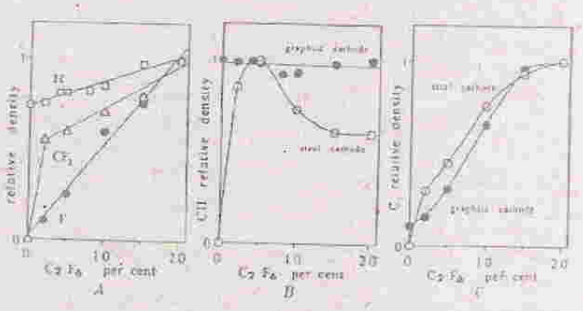

Figure 21. A) Actinometric trends of H, CF_2 and F *vs* C_2F_6 addition. B) and C) trends with graphite and steel cathodes of CH and C, respectively.

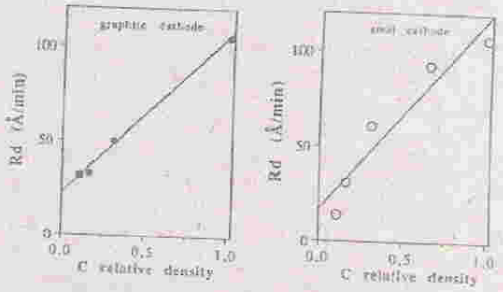

Figure 22. a-C:H,F deposition rate *vs* gas-phase C-atom density for graphite and steel cathodes.

If we compare these data with the profiles of deposition rate we find a deposition rate linearly increasing with the gas-phase density of C-atoms, as unambiguously shown in figure 22 both for the graphite and the steel cathode cases. This result fairly well agrees with an active role of C-atoms as precursors for the deposition process. The intercept of figure 22 for the graphite cathode case, then, leads to a role to be attributed to CH radicals when C-atoms are absent (the intercept for the steel cathode case, on the other hand, points to a co-deposition of sputtered iron, as revealed by XPS data). The advantageous feature of this experimental approach which now becomes apparent is that it is possible to switch from a chemistry mainly based on C-atoms as precursors into one based on CH radicals.

In figures 23 it is shown that the extent of fluorination of a-C:H,F films only depends on gas-phase F-atom density. This is another important difference from what it is obtained with feeds containing higher percentages of C_3F_6. In that case, in fact, CF_x radicals with their distribution ruled out the F-to-C ratio in the film.

Finally, it is interesting to notice that in this case also ion bombardment can have both an activating effect and a deactivating one, depending on their energy, as it is shown in Figure 24

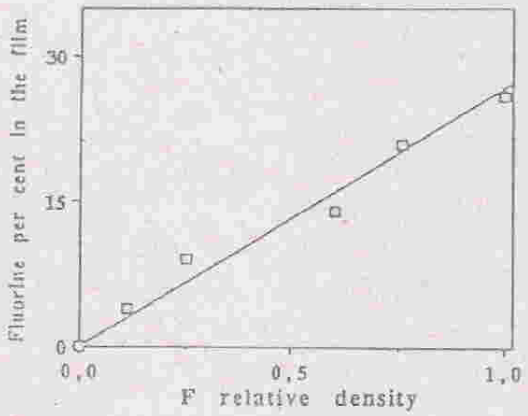

Figure 23. XPS fluorine percentage in the Film *vs.* gas-phase F-atom density.

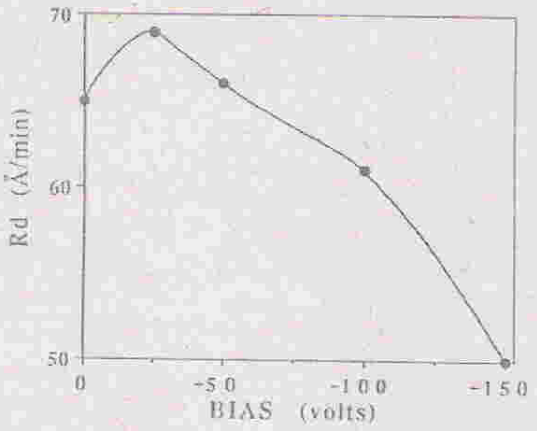

Figure 24. a-C:H,F deposition rate *vs.* bias voltage.

It can be concluded that a-C:H,F films from (0-20%) C_2F_6-H_2 mixtures are formed by two parallel routes, one promoted by C-atoms and the other one by CH-radicals. The extent of fluorination depends only on the gas phase density of fluorine. The overall deposition rate is the result of the competition of ion assisted deposition and ion sputter-assisted-etching processes.

REFERENCES

1) d'Agostino R., Cramarossa F., Fracassi F., Illuzzi F., Caporiccio G., European Patent Application no. 230993 (1987).
2) d'Agostino R., Cramarossa F., Fracassi F., De Simoni E., Sabbatni L., Zambonin P.G., Caporiccio G., Thin Solid Films, 243, 163 (1986).
3) Lamendola R., Favia P., d'Afgostino R., submitted for publication.
4)d'Agostino R., Capezzuto P., Bruno G., Cramarossa F., Pure Appl. Chem., 57, 1287 (1985).
5) Yasuda H.K., in: "Thin Film Processes", Vossen J.L., Kern W. eds., Academic Press, (1978), and refs. therein.
6) d'Agostino R., unpublished results.
7) Yasuda H.K., "Plasma Polymerization", Academic Press (1985).
8) Kammermaier J., Rittmayer G., Schulte R., Proc. of the 6th Int.Symp. on Plasma Chemistry ISPC-6, Montreal (1983).
9) Kammermaier J., Rittmayer G., Proc. of the 7th Int. Symp. on Plasma Chemistry ISPC- 7, Eindhoven (1985).
10) Carmi U., Inspector A., Avni R., Plasma Chem. Plasma Proc., 1, 233 (1981).
11) Claude R., Moisan M., Wertheimer M.R., Zakrzewski Z. in "Polymeric Materials Science and Engineering", Shen M., Bell A.T. eds., Proc. of the ACS Division of Polymeric Materials, 56, Denver (1987).
12) Claude R., Moisan M., Wertheimer M.R., Zakrzewski Z., Appl. Phys. Lett., 50, 1797 (1987).
13) Claude R., Moisan M., Wertheimer M.R., Zakrzewski Z., Plasma Chem. Plasma Proc., 7, 451 (1987).
14) Wertheimer M.R., Moisan M., J. Vac. Sci. Technol., A3, 2643 (1985).
15) Ferreira C.M., J.Loureiro, J.Phys. D., 17, 1175 (1984).
16) Vossen J.L., J. Electrochem. Soc., 126, 1308 (1978).
17) Yasuda H., Hsu T., Surface Science, 76, 232 (1978).
18) Rice D.W., O'Kane D.F., J. Electrochem. Soc., 123, 1308 (1976).
19) Ohki Y., Nakano T., Yahagi K., Proc. of the 7th Int. Symp. on Plasma Chemistry ISPC-7, Eindhoven (1985).
20) Koenig H.R., Maissel L.I., IBM J. Res. Develop., 14, 168 (1970).
21) Coburn J.W., Kay E., J. Appl. Phys., 43, 4965 (1972).
22) Koler K., Coburn J.W., Horne D.E., Kay E., Keller J.H., J.Appl. Phys., 57, 59 (1985).
23) Bruce R.H., J. Appl. Phys., 52, 7064 (1981).
24) Coburn J.W., Winters H.F., J.Vac. Tecnol., 16, 391 (1979).
25) Fracassi F., Occhiello E., Coburn J.W., J.Appl. Phys., 62, 3980 (1987).
26) Christensen O., Jensen P., J.Phys. E 5,86 (1972).

27) d'Agostino, R., Cramarossa F., Fracassi F., Illuzzi F. I. "Plasma Deposition, Treatment and Etching of Polymer Films", d'Agostino R. ed., Academic Press (1990).
28) Fracassi F., Coburn J.W., J. Appl. Phys. 63 (5), 1 (1988).
29) d'Agostino R., Favia P., Fracassi F., J. Pol. Sci. A: Pol. Chem., 28, 3387 (1990).
30) d'Agostino R., Cramarossa F., De Benedictis S., Plasma Chem. Plasma Proc. 2. 213 (1982).
31) d'Agostino R., Cramarossa F., De Benedictis S., Fracassi F., Plasma Chem. Plasma Proc., 4, 163 (1984).
32) d'Agostino R., Cramarossa F., Fracassi F., Laska L., Masek K., Plasma Chem. Plasma Proc. 5, 239 (1985).
33) d'Agostino R., De Benedictis S., Cramarossa F., Plasma Chem. Plama Proc., 4, 1 (1982).
34) d'Agostino R., Colaprico V., Cramarossa F., Plasma Chem. Plasma Proc., 1, 365 (1981).
35) Donnelly V. M., Flamm D.L., Doutremont-Smith W.C., Weder D.J., J.Appl. Phys. 55, 5974 (1984).
36) Coburn J.W., Winter H.F., J. Vac. Sci. Techn., 16, 391 (1979); Kay E., Coburn J.W., Dilks A., in: "Topics in Current Chemistry", Veprek S., Venugopalan M. eds., Plasma Chemistry III, 94, Springer-Verlag, Berlin (1980).
37) Pittman A.G., in "Fluoropolymers" (L.A. Wall ed.), Wiley, New York (1972).
38) Momose Y., Takada T., Okagaki S, in: Polymeric Materials Science and Engineering", Shen M., Bell A.T. eds., Proc. of ACS Division of Polymeric Materials, 56, Denver (1987).
39) Coburn J.W., Chen M., J. Appl. Phys., 51, 3134 (1980).
40) d'Agostino R., Cramarossa F., De Benedictis S., Ferraro G., J. Appl. Phys., 52, 1259 (1981).
41) d'Agostino R., Cramarossa F., De Benedictis S., Fracassi F., Plasma Chem. Plasma Proc., 4, 163 (1984).
42) d'Agostino R., Cramarossa F., Colaprico V., Plasma Chem. Plasma Proc., 1, 365 (1981).
43) d'Agostino R., Cramarossa F. De Benedictis S., Plasma Chem. Plasma Proc. 4, 21 (1984).
44) d'Agostino R., Cramarossa F., Illuzzi F., J.Appl. Phys., 61, 2754 (1987).
45) d'Agostino R., Proc. of XVI ICPIG, invited, Dusseldorf (1983).
46) Dilks A. in: "XPS for Investigation of Polymeric Materials", Brundle C.R., Baker A.D. Eds., Electron Spectroscopy 4, Acad. Press, London (1981).
47) Clark D.T., in: "Esca Appl. to Organic and Polymeric Systems", Briggs D., ed., Handbook of X-Ray and UV Photoelectrn Spectroscopy, Heydem. London (1978).
48) Dilks A., Kay E., Macromolecules, 14, 855 (1980).
49) Kay E., Z. Phys. D., 3, 251 (1986).
50) Biederman H., Vacuum, 37, 367 (1987).
51) Biederman H., Martinu L., Slavinska D., Chudacek I., Pure Appl. Chem. 60, 607 (1988).
52) Kay E., Dilks A., Hetzler U., Macromol. Chem. A. 12, 1393 (1978).
53) d'Agostino R., Martinu L., Pische V., Proc. of 9th Int. Symp. on Plasma Chemistry ISPC-9, Pugnochiuso, Italy (1989).
54) Martinu L., Biederman H., Plasma Chem. Plasma Proc., 5, 81 (1985).
55) Martinu L., Spatenka P., Biederman H., Sicha M., Thin Solid Films, 141, L83 (1986).
56) Kay E., Coburn J., Dilks A., in: "Topics in Current Chemistry", 94, 1 (1981).
57) Martinu L., Biederman H., Vacuum, 36, 477 (1986).
Despax B., Hanchett V., Kay E., J. Vac. Sci. Tec. A. 4, 46 (1986).
58) Martinu L., Solar Energy Materials, 15, 135 (1987).
59) Perrin J.,theimer in: "Plasma Deposition, Treatment, and Etching of Polymers", R. d'Agostino ed., Acad. Press (1990) and refs. therein.
60) Beale H.A., Ind. Res. Develop., 23, 135 (1981).
61) Biederman H., Vacuum, 34, 405 (1984).
62) Mannini A., Bagnoli P., Dilligenti A., Neri ., Pugliese S., J. Appl. Phys., 62, 2138 (1987).
63) Morita S., Hattori S., Pure Appl. Chem., 57, 1277 (1985).
64) Hori M., Yasuda T., Yamada H., Morita S., Hattori S., Plasma Chem. Plasma Proc., 7, 155 (1987).
65) Kay E., Proc. E-MRS Meeting, 15, 355 (1987).
66) A.M. Wrobel, M.R. Wer
67) Favia P., Colaprico V., Fracassi F., De Santis C., d'Agostino R., Proc. of the Meeting on Sintesi e Methodologie Speciali in Chimica Inorganica, Bressanone, Italy (1991).
68) Fracassi F., Favia P., d'Agostino R., J. of Electrochem. Soc., in press.
69) Favia P., Fracassi F., d'Agostino R., J. Biomat. Sci.: Polym. Eds., in press.
70) Favia P., Lamendola R., d'Agostino R., Plasma Sour. Sci. Tech., 1, 59 (1992).
71) Favia P., Caporiccio G., d'Agostino R., work in preparation.
72) Favia P., Fracassi F., d'Agostino R., Proc of 9th Symp. on Elementary Processes and Chemical Reactions in Low pressure Plasma, invited, Casta (Czekoslovaki) 1992.
73) Angus J.C., Koidl P., and Domitz S. in: "Plasma Deposited Thin Films" Mort J., and Jansen F., Eds. (CRC Press, Boca Raton) (1986).
74) Catherine Y. to be published in: "Diamond and Diamond-like Films and Coatings" Angus J., Clausing R., Horton L., Koidl P., Eds., NATO-ASI Series, Plenum, New York (1990).
75) Aisemberg S., J. Vac. Sci. Technol., A 2, 369 (1984).
76) Koidl P., Wild C., Dischler B., Wagner J., and Ramsteiner M., Material Science Forum 52-53, 41 (1989).
77) Angus J.C., and Hyman C.C., Science, 241, 913 (1988).
78) Messier R., Badzian A.R., Badzian T., Spear K. E., Bachmann P., and Roy R. 1987, Thin Solid Films, 153, 1 (1987).
79) Hsiao-Chu Tsai, Bogy D.B., J. Vac. Sci. Technol., A 5(6), 3287 (1987).
80) Koidl P., Wild C., Locher R., and Sah R.E., to be published in: "Diamond and Diamond-like Films and Coatings", Angus J., Clausing R., Horton L., Koidl P., Eds. NATO-ASI Series Plenum, New York (1990).